Atmospheric Pollution Research
www.atmospolres.com

Comparative evaluation of the impact of WRF–NMM and WRF–ARW meteorology on CMAQ simulations for O_3 and related species during the 2006 TexAQS/GoMACCS campaign

Shaocai Yu, Rohit Mathur, Jonathan Pleim, George Pouliot, David Wong, Brian Eder, Kenneth Schere, Rob Gilliam, S. Trivikrama Rao

Atmospheric Modeling and Analysis Division, National Exposure Research Laboratory, U.S. Environmental Protection Agency, Research Triangle Park, NC 27711

ABSTRACT

In this paper, impact of meteorology derived from the Weather, Research and Forecasting (WRF)– Non–hydrostatic Mesoscale Model (NMM) and WRF–Advanced Research WRF (ARW) meteorological models on the Community Multiscale Air Quality (CMAQ) simulations for ozone and its related precursors has been comparatively evaluated over the eastern United States using surface network (AIRNow) data and over the Texas area with the intensive observations obtained by NOAA aircraft P–3 flights and ship during the 2006 TexAQS/GoMACCS campaign. The NMM–CMAQ and ARW–CMAQ models were run on the basis of their original grid structures of the meteorological models. The results at the AIRNow surface sites showed that the model performance for ARW–CMAQ and NMM–CMAQ models was similar and reasonable for the high maximum 8–hr O_3 concentration range (>40 ppbv) with slightly better performance for ARW–CMAQ [the normalized mean bias (NMB) values of ARW–CMAQ and NMM–CMAQ are 8.1 and 9.4%, respectively]. The results of the evaluation using aircraft observations over the Houston–Galveston–Brazoria and Dallas metropolitan areas revealed that both models had similar performances for different chemical species (O_3, CO, PAN, NO_2, NO, NO_X, HNO_3, NO_Y and ethylene) as both models use the same chemical mechanism and emissions. Both models reproduced the vertical variation patterns of the observed air temperature and water vapor well with the slightly lower values for the ARW–CMAQ model. The evaluation results with ship observations over the Gulf of Mexico showed that both models captured, with a good deal of accuracy, the temporal variations and broad synoptic change seen in the observed O_3, NO_Y, CO and O_3+NO_2 with the mean NMB value <25% most of the time.

Keywords:
Air quality
Modeling
Emission
Ozone
Meteorology

Article History:
Received: 28 August 2011
Revised: 04 November 2011
Accepted: 23 November 2011

Corresponding Author:
Shaocai Yu
Tel: +1-919-541-0362
Fax: +1-919-541-1379
E-mail: yu.shaocai@epa.gov

doi: 10.5094/APR.2012.015

1. Introduction

Ozone (O_3), a secondary pollutant, is created in part by pollution from anthropogenic and biogenic sources through a complex series of photochemical reactions involving many volatile organic compounds (VOC) and nitrogen oxides (NO_x). The Clean Air Act and its Amendments require that the US Environmental Protection Agency (EPA) establish National Ambient Air Quality Standards (NAAQS) for O_3. To address human health concerns associated with ground–level O_3, the U.S. EPA declared the daily maximum 8–hr O_3 NAAQS concentration not to exceed 0.085 ppm in 1997 (EPA, 1999). On March 27, 2008, EPA revised the primary and secondary standards for the daily maximum 8–hr O_3 to 0.075 ppm to provide requisite protection of public health and welfare, respectively (Federal Register, 2008). The rationale for this revision includes consideration of: (1) evidence of health effects related to short–term exposure to O_3; (2) insights gained from quantitative exposure and health risk assessments; (3) public and the Clean Air Scientific Advisory Committee (CASAC) Panel comments (Federal Register, 2008). This final rule has been in effect since May 27, 2008. This rule led to more regions in the U.S. with daily maximum 8–hr O_3 concentrations exceeding the level of the revised NAAQS than the old standard.

Harmful levels of O_3 are widely observed under slowly moving, and stagnating, high pressure systems, hot and clear atmospheric conditions at locations downwind of VOC and NO_x emissions. Over the northeastern U.S, the high O_3 episodes are associated with a classic "transitional anticyclone" scenario in which clean, cold–core continental polar air mass transitions, through continued subsidence, into a warm–core, mixing–limiting air mass that is conducive to the formation of O_3 (Eder et al., 1994; Yu et al., 2007; Zhang et al., 2009). In contrast, in southern urban areas such as Houston, Texas, the maximum O_3 is associated with either the frontside of migrating anticyclones, or the backside of migrating anticyclones which are more prevalent during the relative cooler months of April, May, September and October (Davis et al., 1998). As analyzed by Bao et al. (2005) and Banta et al. (2005), the re–circulation and convergence of ozone and its precursors by the sea–breeze can enhance surface O_3 concentrations and cause high O_3 episodes in the Houston area.

One of the most important components of air quality models (AQMs) is the prognostic meteorological model, which generates the three–dimensional meteorological fields required for the chemistry and atmospheric transport simulations. The influence of meteorological conditions on ozone exceedance events has been examined by Pagnotti (1987) and Biswas and Rao (2001). By examining the uncertainty associated with photochemical modeling using the Variable–Grid Urban Airshed Model (UAM–V) with two different prognostic meteorological models [e.g., the Regional Atmospheric Modeling System (RAMS) and Fifth–Generation NCAR/Penn State Mesoscale Model (MM5)], Biswas and Rao (2001) found that neither modeling system performed

significantly better than the other in reproducing the observed O_3 concentrations. The Weather, Research and Forecasting (WRF) model, a next generation mesoscale weather model, has been used to provide meteorological input for the Community Multiscale Air Quality (CMAQ) model. There are two dynamic cores within the WRF framework: the Non–hydrostatic Mesoscale Model (NMM) developed by NCEP (Janjic, 2003) and the Advanced Research WRF (ARW) developed by NCAR (Skamarock et al., 2005). The WRF model is designed to provide a common framework for both operational numerical weather prediction and atmospheric research. The WRF–NMM focuses on operational aspects while the WRF–ARW focuses on research study. Based on an evaluation of these two models from two high–impact weather events during the winter season over Colorado, Szoke et al. (2007) found that there was clearly more precipitation in the WRF–ARW (maximum of 2–2.5 inches) than the WRF–NMM (1.75–2 inches). Overall, the WRF–ARW was the better forecast, with the larger area of heavier precipitation being closer to the observed amounts (Szoke et al., 2007). The WRF–NMM model is the successor of the NCEP Eta model, which has been linked to the CMAQ modeling system (Otte et al., 2005). This Eta–CMAQ model started to operationally forecast O_3 in June of 2004 for different domains in USA (Eder et al., 2006; Yu et al., 2007). In 2006, the Eta model was replaced with the WRF–NMM model to provide the meteorological fields for the CMAQ model. Compared to the Eta model, the ARW–NMM has the following three major improvements: (1) conform to the WRF data interface infrastructure, (2) adoption of 60 levels, upper–levels pressure–surfaces and lower–levels with a terrain following sigma–pressure hybrid coordinate, (3) non–hydrostatic approach.

The Houston–Galveston–Brazoria metropolitan area has a high density of petroleum refineries, synthetic organic chemical manufacturing plants and various mobile sources, and is distinguished by the largest concentration of petrochemical industrial facilities in the U.S. Due to these sources, this area is characterized by a high diversity of emissions of VOCs, CO and NO_X, especially along the Houston Ship Channel. In addition, one of the largest electric utility power plants in the nation, the W.A. Parish facility, is located just outside of Houston. In the study of the Houston urban plumes and petrochemical (Ship Channel) dominated plumes from the previous TexAQS 2000 campaign, Wert et al. (2003) found that petrochemical ethylene and propene emissions could alone account for the general rate and magnitude of extremely high O_3 (245 ppbv) and HCHO (32 ppv) concentrations observed in the Ship Channel plumes on 1 September 2000.

The 2006 Texas Air Quality Study/Gulf of Mexico Atmospheric Composition and Climate Study (TexAQS/GoMACCS) was conducted during August 1 and October 15, 2006. The purpose of the study is to provide a better understanding of the sources and atmospheric processes responsible for the formation and distribution of ozone and aerosols in the atmosphere, their impact on human health and regional haze as well as the influence on the radiative forcing of climate over Texas and the northwestern Gulf of Mexico. This 2006 experiment resulted in a comprehensive set of measurements of chemical composition and meteorological variables, both from surface (ground sites and ship) and aircraft based platforms. These data can be used to examine in detail the performance of AQMs from a multi–pollutant perspective, in terms of their surface concentrations as well as vertical distributions, helping to identify deficiencies in existing models and provide guidance for further model enhancements/improvements.

In this study, the WRF–NMM and WRF–ARW models are used to supply meteorological input to the CMAQ model. The objective of this study is to evaluate the impact of the meteorological fields generated by these two models on the CMAQ simulations for O_3 and its related precursors. The purpose of this paper is twofold. First, this study comparatively examines the impact of these two different meteorological fields on CMAQ simulations for vertical profiles of O_3 and its precursors on the basis of the extensive measurements obtained by aircraft and ship during the 2006 TexAQS/GoMACCS field experiment, especially, for three plumes produced by power plant, Houston and Dallas urban and Ship Channel over the Houston–Galveston–Brazoria (HGB) and Dallas–Fort Worth (DFW) metropolitan areas. Second, the influence of these two different meteorological fields on spatial and temporal variations of O_3 over the eastern U.S. is evaluated against the observations from the AIRNow surface monitoring network.

2. Description of the Modeling System and Observational Databases

2.1. Description of the modeling system

Since deployed during the summer of 2004, the Eta–CMAQ air quality forecasting system (Otte et al., 2005), created by linking the Eta model (Rogers et al., 1996) and the CMAQ (Byun and Schere, 2006), started to provide air quality forecasts over the different domains (Eder et al., 2006; Eder et al., 2009). The Eta–CMAQ model performance for O_3 and $PM_{2.5}$ was comprehensively assessed with observations obtained during the 2004 ICARTT field experiment (Yu et al., 2007; Yu et al., 2008). In 2006, the Eta model was replaced with the WRF–NMM model to provide the meteorological fields for the CMAQ model to operationally forecast O_3. The WRF model is a new state–of–science mesoscale model framework. It has become popular for various applications in the air quality community. Two dynamic cores are available within the WRF framework: NMM and ARW. The NMM core is a fully compressible hydrostatic NWP (Numerical Weather Prediction) model using mass based vertical coordinate, which has been extended to include the non–hydrostatic motions (Janjic, 2003). The NMM core uses a terrain–following hybrid (sigma–pressure) vertical coordinate and Arakawa E–grid staggering for the horizontal grid. The ARW core is a fully compressible, Eulerian nonhydrostatic model with a run–time hydrostatic option available. This core uses a terrain–following hydrostatic–pressure vertical coordinate with vertical grid stretching and Arakawa C–grid staggering for the horizontal grid.

In contrast to the Eta–CMAQ modeling system, WRF–NMM/CMAQ (NMM–CMAQ thereafter) uses the lowest 22 layered vertical grid structure of the 60 hybrid layers in WRF–NMM meteorological fields directly without vertical interpolation through the use of a common vertical coordinate system. The interface processor, PREMAQ (CMAQ preprocessor), was modified to post–process meteorological fields (for use by CMAQ) on the vertical grid and coordinate system used by the WRF–NMM. The updated processor code also reads data on the native WRF–NMM layer structure (currently 60 between the surface and 2 mb) and performs the necessary calculations to transform them to a chosen number of few layers (the lowest 22 layers in this study) for the CMAQ simulations. These modifications enable the CMAQ calculations to be made on the same vertical coordinate and grid structure as the WRF–NMM and provide consistent coupling between the two modeling systems. On the other hand, for non–forecast (historical) applications, the WRF–ARW model has been employed to generate meteorological fields for CMAQ (WRF–ARW/CMAQ) (ARW–CMAQ thereafter) because the WRF–ARW meteorological model is compatible with CMAQ like MM5 before. In this study, both NMM–CMAQ and ARW–CMAQ are run during the 2006 TexAQS/GoMACCS period. Table 1 lists the setup of NMM and ARW dynamical cores, which are exercised with their own sets of physics. The version 3.0 of ARW is used in this study (Gilliam and Pleim, 2010). In terms of the NMM–CMAQ run, this study uses the results from the target forecast period (0400 Coordinated Universal Time (UTC) to next day's 0300 UTC) based on the 1 200 UTC NMM–CMAQ simulation cycle over the domain of the continental United States (see Figure 1a). In contrast, the ARW–CMAQ model was applied over a domain encompassing the eastern United States (see Figure 1b) and was run continuously over the whole period. In both models, the lateral boundary

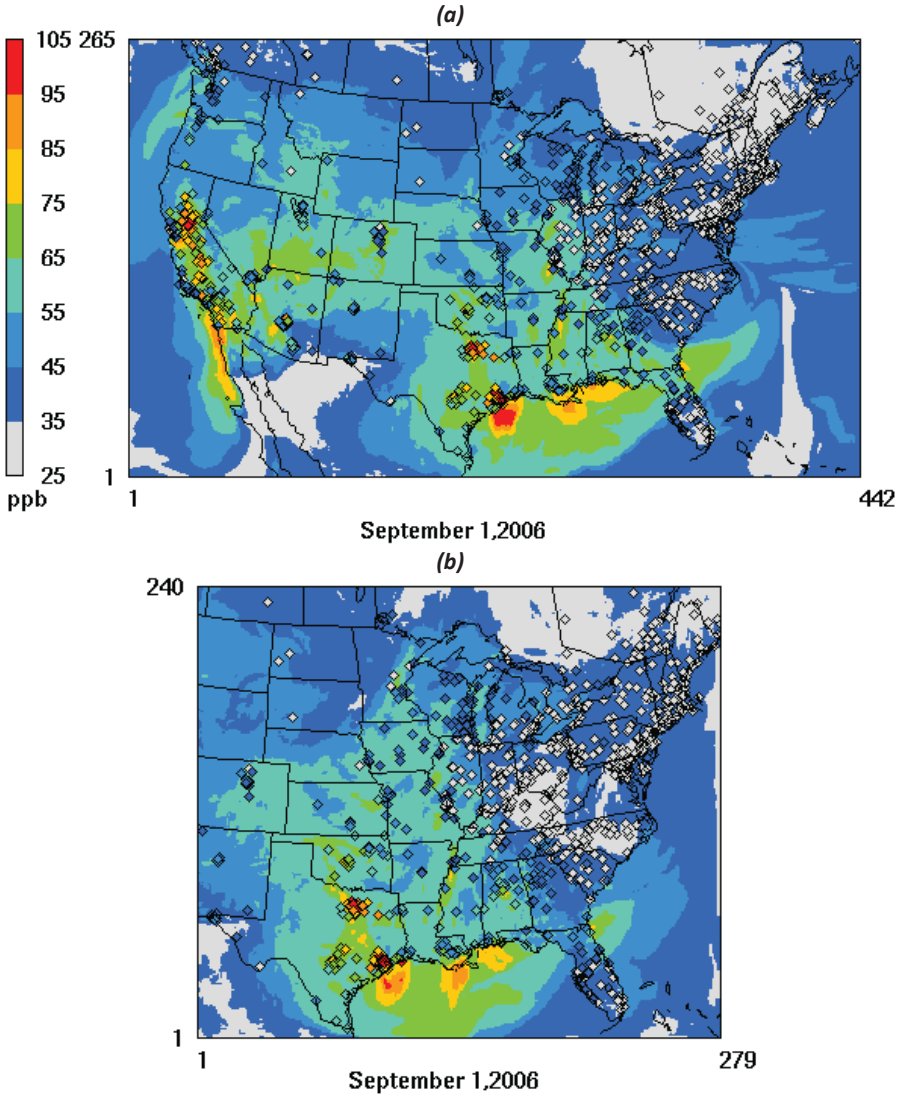

Figure 1. *The model domains of* ***(a)*** *NMM–CMAQ and* ***(b)*** *ARW–CMAQ. The model simulation results for maximum 8–hr O_3 concentrations (ppbv) with AIRNow observed data overlaid (diamond) on 1 September, 2006 are also shown in the figures. "442", "265", "279" and "240" are grid cell number.*

Table 1. *Setups of the WRF–ARW and WRF–NMM meteorological models*

	WRF–ARW	WRF–NMM
Land–Surface Model	PX	NOAH unified 5 layer
Planetary Boundary Layer	ACM2	MYJ (Mellor–Yamada–Janjic) 2.5
Cloud Microphysics	Thompson	Ferrier
Cumulus Parameterization	KF2	Betts–Miller–Janjic convective mixing scheme
Shortwave	Dudhia	Lacis–Hansen
Longwave	RRTM	Fels–Schwartzkopf
Projection	Lambert Conformal	Rotated Lat–Lon
Grid Staggering	C	E
Vertical Coordinate	Terrain following sigma	Hybrid: terrain following sigma at low levels and isobaric above
Horizontal Grid Spacing	12 km	12 km
Number of verticals levels	34	22
Initial Conditions	NAM–218	NAM–218
Boundary Conditions	NAM–218	NAM–218

conditions are horizontally constant and are specified by continental ''clean'' profile for O_3 and other trace gases; the vertical variations are based on climatology (Byun and Schere, 2006). For both models, the thickness of layer 1 is about 38 m and the vertical coordinate system resolves the atmosphere between the surface and 50 hPa although each model uses different number of vertical levels as seen in Table 1.

The emissions used in the NMM–CMAQ forecasting system are the same as those for the Eta–CMAQ described by Otte et al. (2005). The area source emissions are based on the 2001 National

Emission Inventory (NEI). The point source emissions are based on the 2001 NEI with SO_2 and NO_x projected to 2006 on a regional basis using the Department of Energy's 2006 Annual Energy Outlook issued in January of 2006. The mobile source emissions were generated by EPA'S MOBILE6 model using 1999 Vehicle Miles Traveled (VMT) data and a fleet year of 2006. Daily temperatures from the NMM model were used to drive the inputs into the MOBILE6 model using a nonlinear least squares relationship described by Pouliot (2005) and Otte et al. (2005). The biogenic emissions are calculated as by Otte et al. (2005) using Biogenic Emissions Inventory System (BEIS) version 3.12. Emissions from wild land fires were represented as a 7–year average and all of these emissions were injected into first model layer. Given the fact that both models use different map projections and grid staggering, it is difficult to make the WRF–ARW grid coverage identical to the WRF–NMM coverage. Several steps are taken to ensure that both the models are set up as consistently as possible so that the comparison of the two models is meaningful. First, the meteorological fields of ARW were padded by 5 cells in both x and y directions around the original meteorological domain when the meteorological fields were processed using Meteorology–Chemistry Interface Program (MCIP) to create the CMAQ–ready files. This helps match the larger NMM domain and smaller ARW domain sizes, and is able to use the emission data from the NMM–CMAQ forecast model. Second, the point source emissions were redistributed to the 34 layers according to the ARW meteorological fields on the basis of those from the NMM–CMAQ model. In addition, the ARW–CMAQ uses the same area sources such as the mobile and biogenic sources as those in NMM–CMAQ. Therefore, the total emission budgets for both models are the same. The Carbon Bond chemical mechanism (version 4.2) (Gery et al., 1989) was applied to represent photochemical reaction pathways in both models.

2.2. Observational databases

The hourly, near real–time O_3 data for 2006 at 614 measure–ment sites in the eastern United States are available from the U.S. EPA's AIRNow network (Figure 1), resulting in nearly 1.2 million hourly O_3 observations for the studied period. In addition, measurements of O_3 vertical profiles, its related chemical species (CO, NO, NO_2, HNO_3, PAN, ethylene), and meteorological parameters (liquid water content, water vapor, temperature, wind speed and direction, and pressure) were carried out by instrumented aircraft (NOAA P–3). The research ship was also deployed as part of the 2006 TexAQS/ GoMACCS field experiment. The detailed instrumentation used and protocols for measurements are described at http://esrl.noaa.gov/csd/2006/fieldops/mobileplatforms.html. The flight tracks and ship movements are presented in Figure 2 (http://esrl.noaa.gov/csd/2006/fieldops/). The results for comparison of the impact of two meteorological models on CMAQ simulations over the eastern U.S. (e.g., ARW domain as shown in Figure 1b) during the period from August 6 to October 6, 2006 are analyzed.

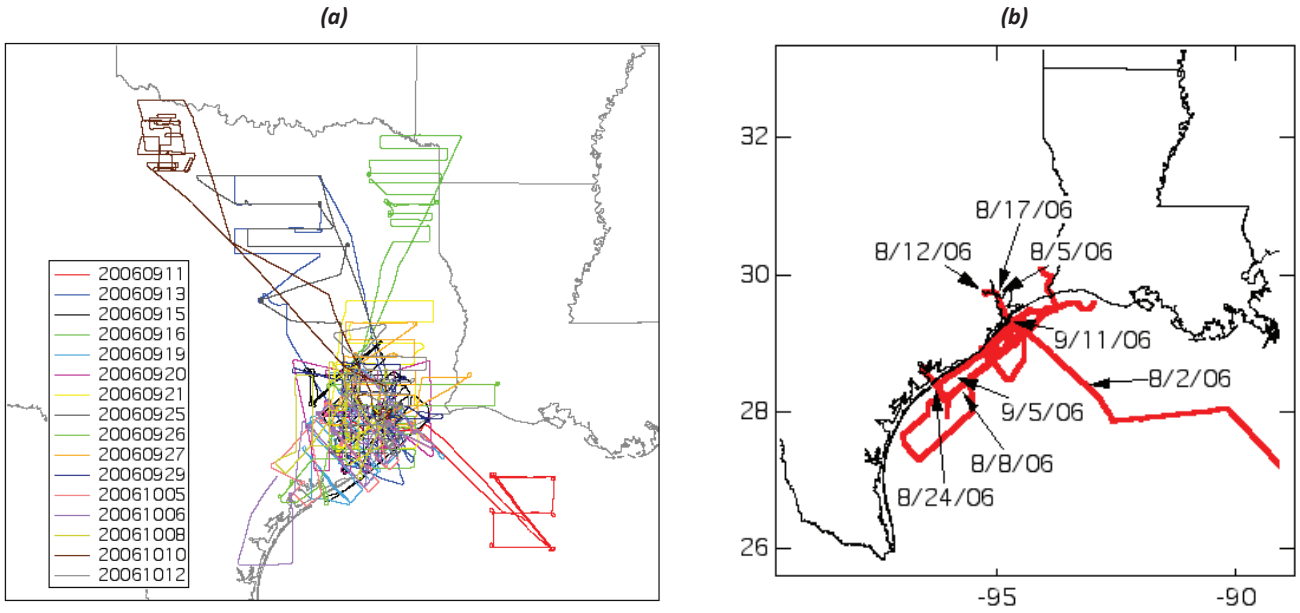

Figure 2. *Tracks of* ***(a)*** *NOAA aircraft P–3, and* ***(b)*** *NOAA Ronald H.* Brown *ship over the Texas during the 2006 TexAQS/ GoMACCS camp.*

Table 2. *Comparison of ARW–CMAQ and NMM–CMAQ models for operational evaluation of maximum 1–hr and 8–hr O_3 concentrations on the basis of the AQS data over the eastern United States. Mean bias (MB), Root mean square error (RMSE), normalized mean bias (NMB), normalized mean error (NME) and correlation coefficient (r). "Domain mean" means the results on the basis of all data at observational sites within the domain*

			Domain Mean, ppbv						
Max O_3,	Model	Data points	Obs	Mod	MB, ppbv	RMSE, ppbv	NMB (%)	NME (%)	r
1–hr	ARW	51 532	48.6	56.2	7.5	13.4	15.5	22.3	0.76
1–hr	NMM	51 532	48.6	56.7	8.1	13.9	16.7	22.8	0.75
8–hr	ARW	51 532	42.7	50.4	7.7	12.6	18.0	24.2	0.76
8–hr	NMM	51 532	42.7	52.0	9.3	13.8	21.8	26.4	0.74
			For O_3>40 ppbv						
1–hr	ARW	33 340	58.1	62.8	4.8	12.2	8.2	16.3	0.61
1–hr	NMM	33 340	58.1	62.7	4.6	11.8	7.9	15.6	0.62
8–hr	ARW	27 563	54.1	58.5	4.4	10.7	8.1	15.6	0.58
8–hr	NMM	27 563	54.1	59.1	5.1	10.7	9.4	15.6	0.57

3. Results and Discussion

3.1. Impact of meteorology on spatial and temporal variations of O_3 over the eastern U.S. domain at the AQS sites

Table 2 summarizes the comparison results of the ARW–CMAQ and NMM–CMAQ for the daily maximum 1–hour and daily maximum 8–hour O_3 concentrations for two groups: one using all data and the other only using an O_3 threshold of 40 ppbv. As can be seen, the Normalized Mean Bias (NMB) and Normalized Mean Error (NME) (Yu et al., 2006a) are 8.1% (9.4%) and 15.6% (15.6%) for ARW–CMAQ (NMM–CMAQ) when only data of maximum 8–hr O_3 with concentrations >40 ppbv are considered, respectively. These values are much lower than the corresponding results when all data are considered, indicating the overestimation in the low O_3 concentration range contributes significantly to the overall overestimation for both models.

Additional insight into the positive bias (over–estimation) and errors (scatter) of both models can be gained from Figure 3a for the scatter plot and Figure 3b for the NMB values as a function of the different observed O_3 concentration ranges. Table 2 and Figure 3 indicate that both models have a very similar good performance for the prediction of high maximum 8–hr O_3 concentrations (>40 ppbv). Figure 3 clearly indicate that both models reproduced the majority of the observed daily maximum 8–hr O_3 with the values>40 ppbv within a factor of 1.5, especially for the concentration range of 60–75 ppbv with the NMB of <1%. However, both models overestimated the observations in the low O_3 concentration range (<40 ppbv) with NMB of 38.9% (ARW–CMAQ) and 48.3% (NMM–CMAQ), respectively. As analyzed by Yu et al. (2007), the overestimation in the low O_3 concentration range could be indicative of titration by NO in urban plumes that the model does not resolve because many AQS sites are located in urban areas. As shown in the analysis below, the NO concen–trations from NMM–CMAQ are lower than those from ARW–CMAQ, leading to more overestimation of low O_3 concentration ranges in NMM–CMAQ relative to those of ARW–CMAQ (see Figure 3). The spatial distributions of NMB values for both models (Figure 3) also show that large overestimation of the observed daily maximum 8–hr O_3 concentrations occurred in northern New England where very low O_3 concentrations were observed.

To estimate the model performance over time, the values of mean, MB, RMSE, NMB, NME and correlation coefficient (r) were calculated (domain wide averages) and plotted as daily time series for the daily maximum 8–hr O_3 as shown in Figure 4. As seen, for the periods with high O_3 (domain–wide mean observed maximum 8–hr O_3>40 ppbv: August 6–24 and September 6–9, 2006), both models have good similar performance with NMB<20% and MB<10 ppbv. In contrast, for the low O_3 concentrations periods, both models consistently overestimated observations by more than 20% in most of time with more overestimations by the NMM–CMAQ.

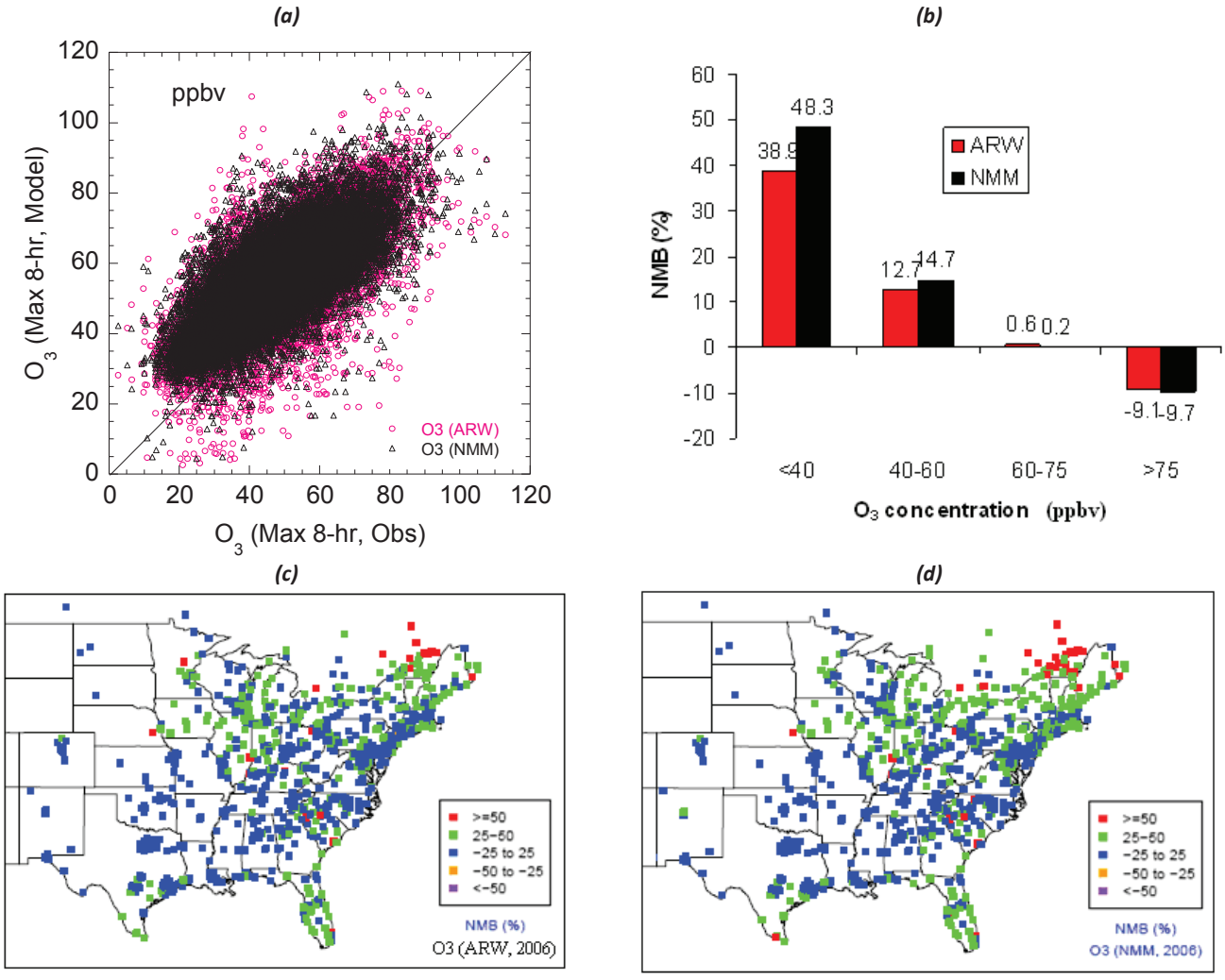

Figure 3. *Comparison of the modeled (ARW–CMAQ, NMM–CMAQ) and observed maximum 8–hour O_3 concentrations at the AIRNow monitoring sites* ***(a)*** *scatter plot (ppbv) (the 1:1 line are shown for reference);* ***(b)*** *The NMB values of each model as a function of the observed maximum 8–hour O_3 concentration ranges; spatial distributions of NMB for* ***(c)*** *ARW–CMAQ and* ***(d)*** *NMM–CMAQ during the period from 5 August to 7 October, 2006.*

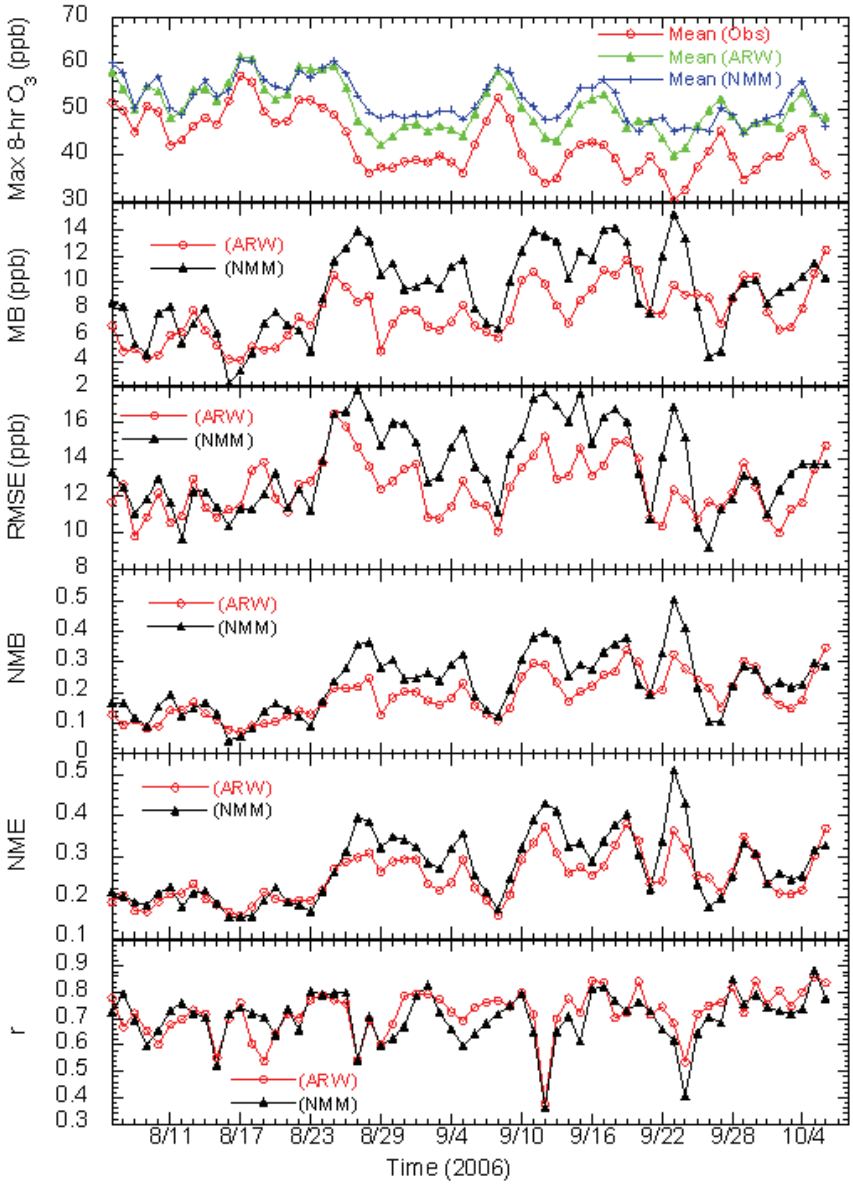

Figure 4. *Time–series of daily variations of the values of domain–wide mean, MB, RMSE, NMB, NME and correlation coefficient (r) for the maximum 8–hour O_3 concentration at the AIRNow monitoring sites for ARW–CMAQ and NMM–CMAQ simulations.*

3.2. Influence of meteorology on vertical profiles for O_3 and its related species, and comparison of meteorological parameters aloft

To compare the modeled and observed vertical profiles, following Mathur et al. (2005) and Yu et al. (2007), the modeled results were extracted by matching the positions of the aircraft to the model grid indices (column, row and layer). The hourly resolved modeled outputs were also linearly interpolated to the corresponding observational times. The observed and modeled data were grouped according to the model layer for each day and each flight; that is, both the observations and predictions were averaged along a particular aircraft transect at an approximate altitude (layer height), representing the average conditions encountered over the study domain. The flight tracks of the aircraft in Figure 2a and Table 3 show that the measurements onboard the P–3 mainly cover the Houston–Galveston–Brazoria metropolitan area except on 8/31, 9/11, 9/13, 9/16, 9/21 and 9/25. All aircraft measurements were conducted in the daytime except on 9/29 as summarized in Table 3 for the flight objectives. Figure 5 presents observed and modeled vertical profiles for O_3, CO, PAN, NO_2, NO, NO_x, HNO_3, NO_y and ethylene on the daily basis during the 2006 TexAQS period. The model performance for NO_z (NO_z = NO_y–NO_x) and O_3 + NO_2 for the daytime hours (6:00 am to 6:00 pm) is shown in Figure 6. Table 4 summarizes the results of comparison for the observations and models for all data. Note that ARW–CMAQ and NMM–CMAQ use 34 and 22 layers, respectively, between the surface and 100 hPa, and only observation results grouped according to the ARW model layer are shown in Figure 5 for observations to avoid overcrowding.

As shown in Figure 5, both models generally reproduce the observed O_3 vertical structure with the better performance in the middle altitude (~800 m) although both models tended to overestimate in the high altitude (>3 000 m) and underestimate in the low altitude (<300 m) (see the mean lines in Figure 5). On the other hand, a noticeable discrepancy is that both models tended to overestimate CO, PAN, NO_x, NO, NO_2, HNO_3, and NO_y at the low altitudes although both models were close to the observations for NO_x, NO, and NO_2 at the high altitude (above 1 000 m) as their concentrations were very low. The mean values of NO_x, NO, NO_2 and NO_y in Table 4 reveal that both models overestimated these

Table 3. *Flight summary for WP–3 aircraft*

Date	Flight objective information [a]
8/31	Transit flight from Tampa, FL to Houston, TX
9/11	Flight over Ronald H. Brown ship and oil platforms in the Gulf of Mexico
9/13	Houston emission characterization and chemical processing
9/15	Houston emissions characterization, Parish power plant emission and chemical processing, winds from the South East
9/16	NE Texas power plants
9/19	Houston urban plume, Parish power plant emission and chemical processing, Ship Channel industrial region for refineries
9/20	Beaumont Port Arthur, Houston urban plume, Parish power plant emission and chemical processing, Ship Channel industrial region for refineries
9/21	Houston urban plume, Parish power plant emission and chemical processing, Ship Channel industrial region for refineries
9/25	Houston, Dallas urban plumes and Parish power plants, Brown and Limestone power plant emission characterization and chemical processing, winds from the North
9/26	Houston urban plume and industrial sources, Parish power plant, Beaumont Port Arthur, Lake Charles emission characterization, chemical processing, winds from the North
9/27	Houston urban plume and industrial sources, Parish power plant emission characterization and chemical processing
9/29	Houston urban plume and industrial sources, Parish power plant emission characterization and chemical processing into night time, light winds from the E switching to the S
10/5	Houston urban plume and industrial sources, Parish power plant emission characterization and chemical processing, light winds from the NE
10/6	Houston urban plume and industrial sources, Parish power plant emission characterization and chemical processing, winds from the NE

[a] *based on flight information presented at: http://esrl.noaa.gov/csd/tropchem/2006TexAQS/P3/FlightSummary/index.php*

Table 4. *Observations and models (NMM–CMAQ and ARW–CMAQ) for different gaseous species (O_3, CO, PAN, NOx, NO, NO_2, HNO_3, NO_y, ethylene, NO_z, air temperature (℃), water vapor (g/kg) and NO_2+O_3 (for lowest 4 layers only)) on the basis of all NOAA P–3 aircraft measurements over the Texas during the 2006 TexAQS (mean ± standard deviation, all units are ppbv except that PAN unit is pptv). Correlations between O_3 and NO_z for the NO_x–limited conditions indicated by the observational data with $(O_3)/(NO_x)>46$ (aged air masses) (see text for explanation)*

	Mean ± standard deviation			NMB (%)	
	Obs	**NMM–CMAQ**	**ARW–CMAQ**	**NMM–CMAQ**	**ARW–CMAQ**
O_3	53.27±17.68	58.27±10.39	56.94±11.39	9.4	6.9
CO	124.05±42.8	118.05±49.24	115.87±48.87	–4.8	–6.6
PAN	448.30±316.8	805.17±556.84	781.99±572.24	79.6	74.4
NO_x	1.51±2.05	3.76±7.05	4.11±8.46	149.0	172.2
NO_2	1.24±1.74	3.15±5.97	3.26±6.44	154.0	162.9
NO	0.24±0.41	0.58±1.26	0.81±2.61	141.7	237.5
HNO_3	1.33±1.12	1.89±1.50	1.79±1.42	42.1	34.6
NO_y	4.61±3.33	9.01±8.17	9.35±9.87	95.4	102.8
Ethylene	0.73±0.87	0.41±0.59	0.40±0.61	–43.8	–45.2
NO_z	2.57±1.70	4.20±2.44	4.01±2.41	63.4	56.0
NO_2+O_3	57.13±26.26	60.71±11.71	60.62±13.39	6.3	6.1
Temperature	20.02±7.18	19.58±7.16	19.09±7.09	–2.2	–4.6
QV	10.13±5.40	9.89±5.32	9.56±4.75	–2.4	–5.6
Obs:	(O_3)=8.4(NOz)+36.9	r=0.65			
ARW–CMAQ:	(O_3)=3.4(NOz)+47.3	r=0.86			
NMM–CMAQ:	(O_3)=2.7(NOz)+50.3	r=0.82			

species by more than a factor of 2. Since the aims of the aircraft observations were to characterize the emission sources from the plumes of the power plant, Houston urban and Ship Channel over the Houston–Galveston–Brazoria metropolitan and Dallas areas as listed in Table 3. The results suggest that the emission inventory used has too high NO_x emissions from these sources over two metropolitan areas. The better model performance for O_3+NO_2 than for O_3 at the low altitudes [below layer 4 (~150 m)] for both models as shown in Figures 5 and 6 (also see Table 4) also reveals that the both models exaggerated the effects of NO titration on O_3. Both models consistently overestimated PAN, HNO_3 and NO_y but underestimated CO at high altitudes as shown in Figure 5. Because ethylene emission is one of reasons for extremely high O_3 (such as 245 ppbv) concentrations observed in the Ship Channel plumes (Wert et al., 2003), the underestimations of ethylene by ~50% by both models (see Figure 5 and Table 4) contributed to the underestimation of O_3 at the lower altitudes. Both models also underestimated biogenic VOC (terpenes and isoprene) systematically by more than a factor of 2 (Yu et al., 2011). Thus, improvement of the NO_x and VOC emission inventories over the Texas region is recommended in order to achieve better model results for these species.

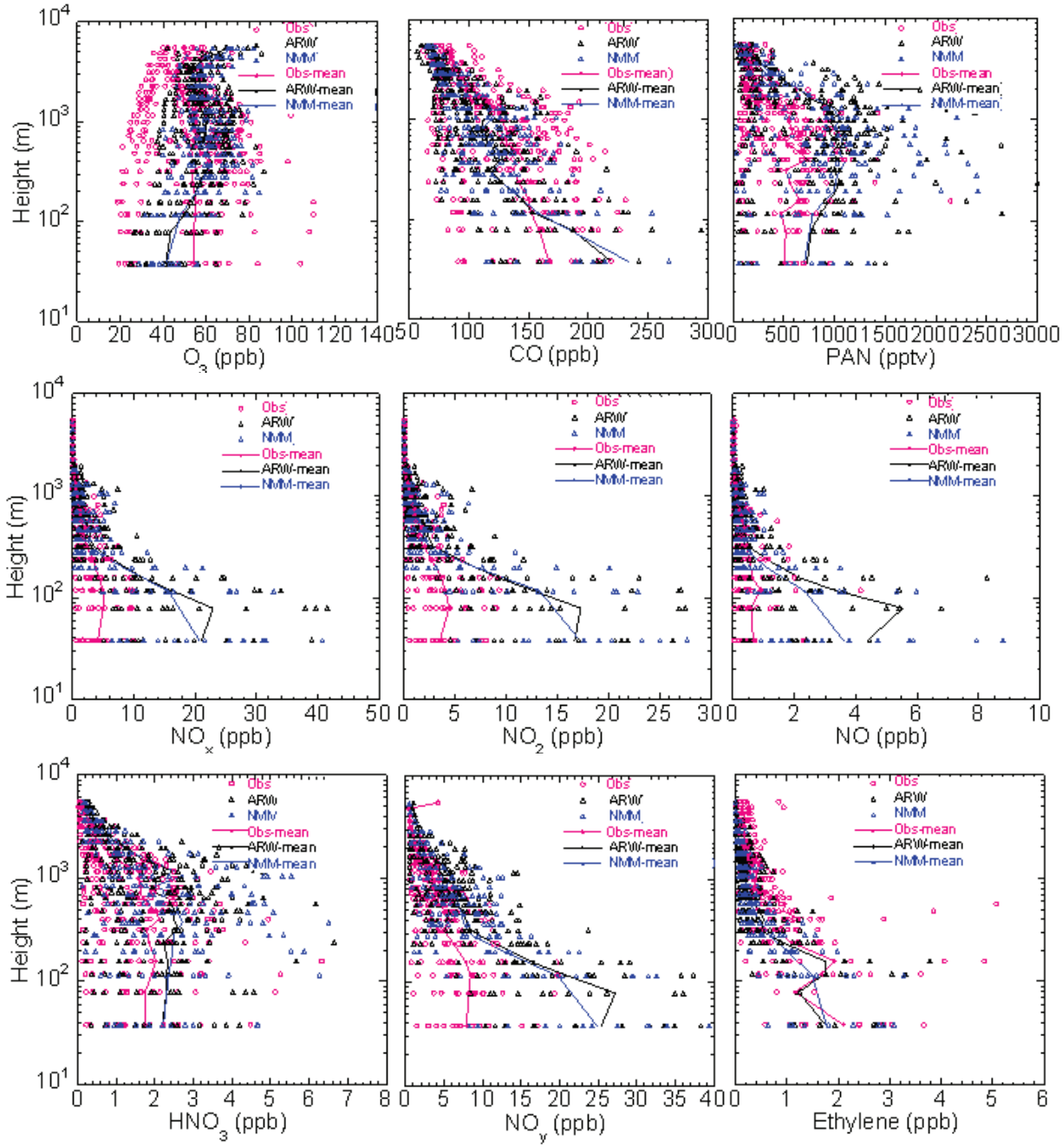

Figure 5. *Vertical O_3, CO, PAN, NO_x, NO_2, NO, HNO_3, NO_y and ethylene profiles for the models and observations from the aircraft P–3 on the basis of daily layer means during 2006 TexAQS. The solid lines represent the means for all data. Note that the logarithmic scale is used for vertical axis.*

Following Arnold et al. (2003) and Yu et al. (2006b), the upper limits of the net ozone production efficiency value (ε_N) can be estimated by the O_3–NO_z slope for models and observational values for the period with the observed $(O_3)/(NO_x)>46$ (aged airmass) during the daytime (6:00 am to 6:00 pm local standard time (LST)) to ensure that the system is well out of the radical–sensitive region of the response surface. Figure 6b and Table 4 indicate that there is significant correlation between O_3 and NO_z for observations and both models ($r>0.68$). The ε_N value for ARW–CMAQ (3.4) is slightly higher than NMM–CMAQ (2.7), and both are ~30% lower than the lower bound of the estimated range (5–10) as shown by Olszyna et al. (1994) at rural sites in the eastern US. In contrast, the observed ε_N value (8.4, see Table 4) is close to the median value of the estimated range of other investigators (Olszyna et al., 1994). Figure 6b also indicates that both models produced less O_3 at the high NO_z regime. The vertical profiles of NO_z in Figure 6a show that the NO_z concentrations for both models were higher than the observations from low to high altitudes (see mean values in Table 4). As pointed out by Yu et al. (2006b), this behavior is because the model chemistry produces more terminal oxidized nitrogen products than inferred from observations, thereby contributing to the noted underestimation of ε_N values. The intercepts (background O_3) from both models are ~10 ppbv higher than the observation. Because both models use the same chemical mechanism and emission, it is reasonable for both models to have similar results as shown in Table 4 and Figures 5 and 6 although NMM–CMAQ has slightly higher concentrations for O_3, CO, PAN, HNO_3, ethylene, and NO_z.

Figure 6c shows that both models reproduced the vertical variation patterns of the observed air temperature and water vapor well, especially for temperature. Specifically, the modeled temperatures are slightly lower than the observations and the mean temperature of the ARW model is slightly lower than that of

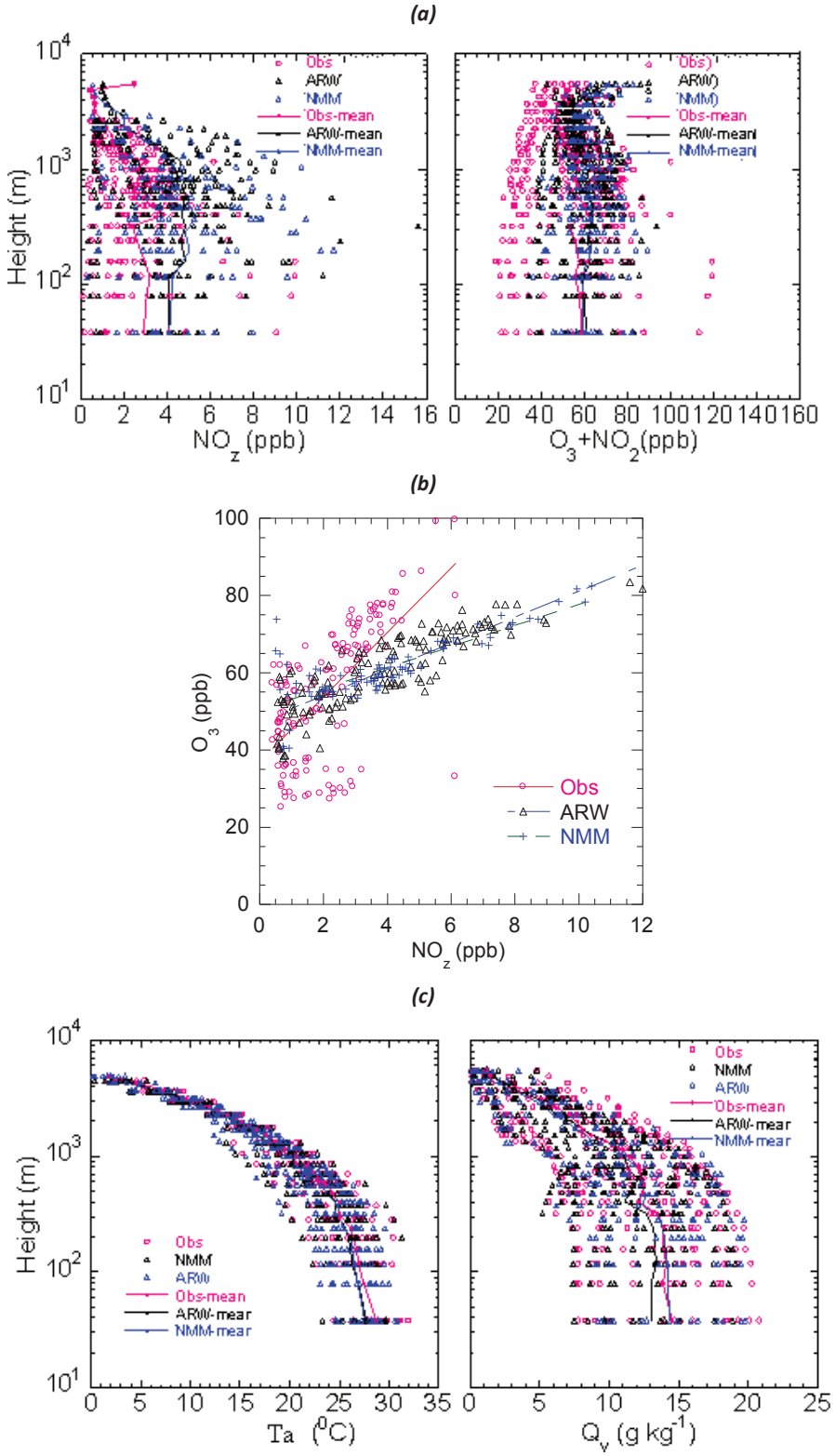

Figure 6. (a) *Comparison of vertical NO_z and O_3+NO_2 profiles for the models and observations (The solid lines represent the meansfor all data);* ***(b)*** *O_3 as a function of NO_z for the NO_x–limited conditions indicated by the observational data with $(O_3)/(NO_y)$>46 (aged air masses) for the models and observations;* ***(c)*** *Comparison of vertical profiles for air temperature (T_a) and water vapor (Q_v). The solid lines represent the means for all data. All results are based on the daily layer means according to the aircraft P–3 measurements during 2006 TexAQ.*

the NMM model (see Table 4). This finding is in agreement with that of Bernardet et al. (2005), who found that the WRF–NMM was consistently half a degree warmer than the WRF–ARW on the basis of the winter forecast experiment of the Development Testbed Center from January to March 2005. This is traced to difference in the initialization method used by meteorological models. On the other hand, both models also underestimated the observed water vapor slightly although the mean water vapor of the NMM model was very close to the observations at the low altitudes as shown in Figure 6c. The water vapor concentrations of the NMM model are also slightly higher than those of the ARW model as indicated in Table 4.

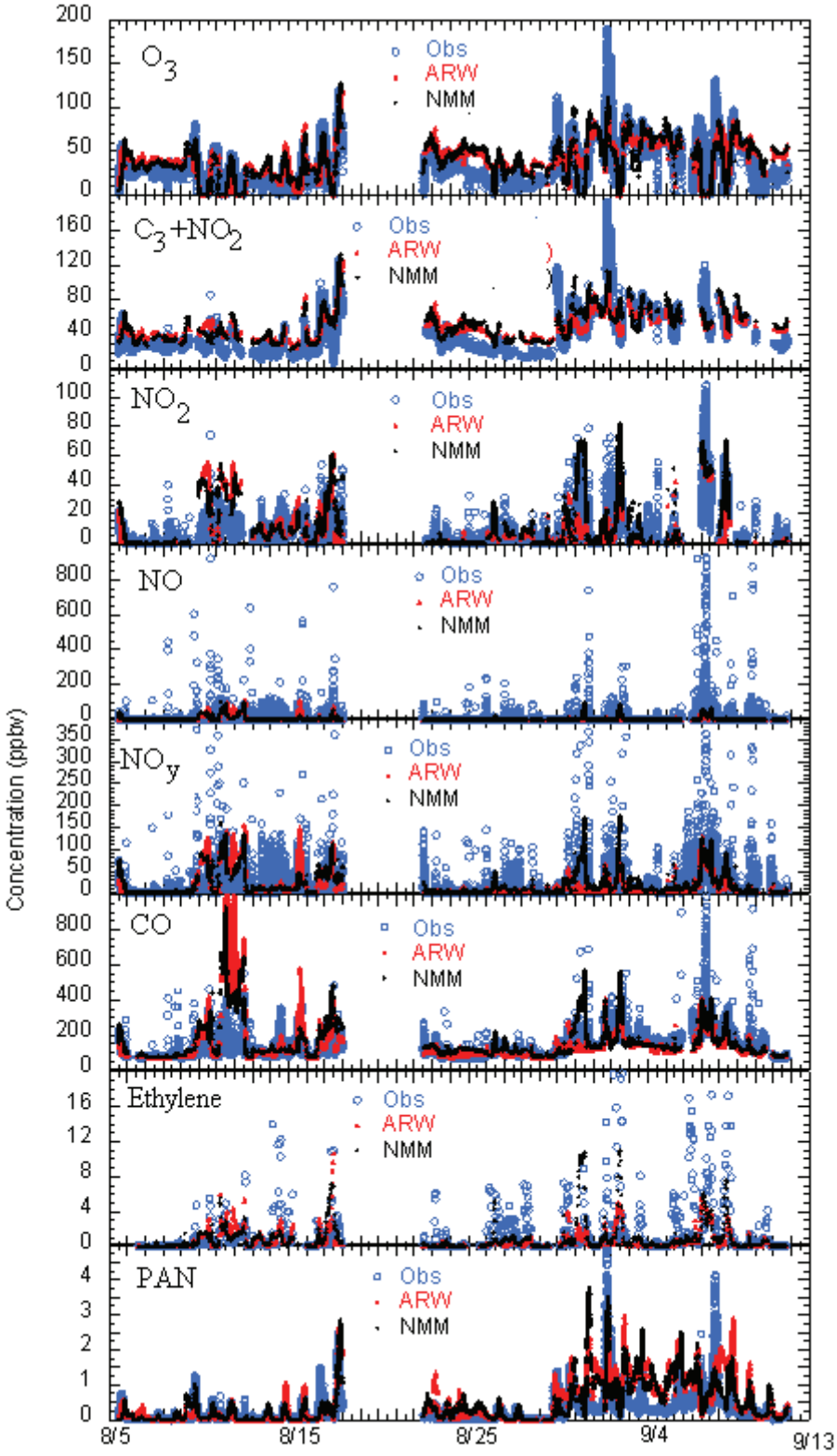

Figure 7. *Time series of observations and model predictions (NMM–CMAQ and ARW–CMAQ) for difference species on the basis of ship measurements over the Gulf of Mexico from 5 August to 13 September, 2006.*

3.3. Time–series comparisons over the Gulf of Mexico with the Ronald H. Brown ship observations

The cruise tracks of the NOAA Ronald H. Brown ship in Figure 2 indicate that most of ship's time was spent sampling along the coast of southeastern Texas over the Gulf of Mexico from August 5 to September 11, 2006. Anthropogenic sources from fossil–fueled electric power plants (such as W.A. Parish, Monticelllo, and Welsh), Houston urban and petrochemical production (such as Ship Channel and Texas City) and biogenic emissions in the region can significantly impact the sampled air masses along the Gulf coast of southeastern Texas. Wiedinmyer et al. (2004) found that approximately 50% of all VOC emissions are of biogenic origin (vegetative emissions) in the urban counties of

the Houston metropolitan area and biogenic emissions may constitute as much as 80% to 90% of the total VOC emissions for the eastern Texas area. Time–series comparisons of observations and models for each parameter (O_3, NO_2, NO, NO_y, PAN, ethylene, temperature, wind speed and direction, and radiation) along the ship tracks (see Fig. 2) during the 2006 TexAQS period are shown in Figures 7 and 8. Note that on 2 September, the NOAA Ship *Ronald H.Brown* was anchored in the Barbour's Cut inlet located off Galveston Bay near Houston Ship Channel, and a rapid increase of O_3 concentrations with peak concentration >150 ppbv was observed.

Figures 7 and 8, and Table 5 indicate that both models captured, with a good accuracy, the temporal variations and broad synoptic change seen in the observed O_3, NO_y, CO, and O_3+NO_2 with the mean NMB value < 25% along the ship track most of the time, although with some occasional major excursions. The improved model performance for O_3+NO_2 than O_3 at low concentrations, especially for late periods after September is shown Figure 7. This finding revealed again that the model has exaggerated the effects of NO titration on O_3 as inferred from the O_3 observations during nighttime over the ocean like those over the land from the previous results with the aircraft. On the other hand, there was a noticeable discrepancy between the observations and models for NO_2, PAN, NO_z and ethylene with the mean NMB value >40% (see Table 5). The coastal region actually is a transition zone between the maritime boundary layer with the relatively constant 600–m mixed layer depths over the Gulf of Mexico and deeper daytime mixed layers inland. This complexity over the coastal region of the Gulf of Mexico causes the model to be unable to simulate the transport well over the land–ocean interface. One of the possible reasons for the large model overestimations for coastal grid cells is that the model's boundary layer mixing cannot resolve steep subgrid land–to–sea gradients (Yu et al., 2007).

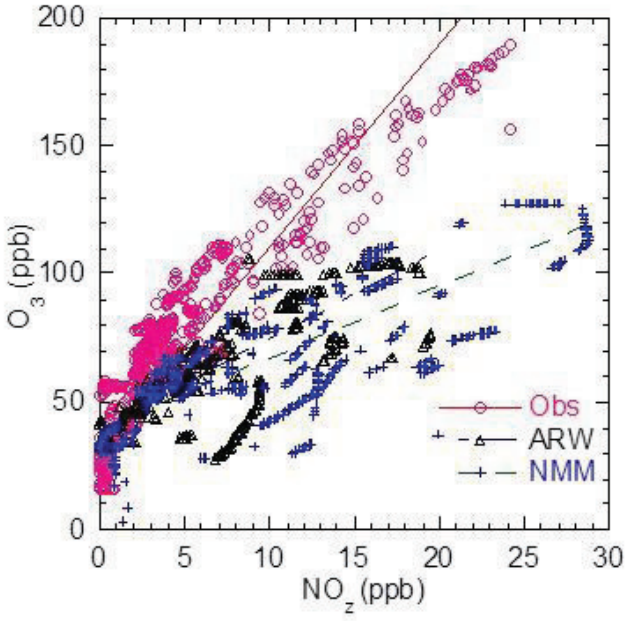

Figure 8. *O_3 as a function of NO_z for the NO_x–limited conditions indicated by the observational data with $(O_3)/(NO_x)$>46 on the basis of ship measurements from 5 August to 13 September, 2006.*

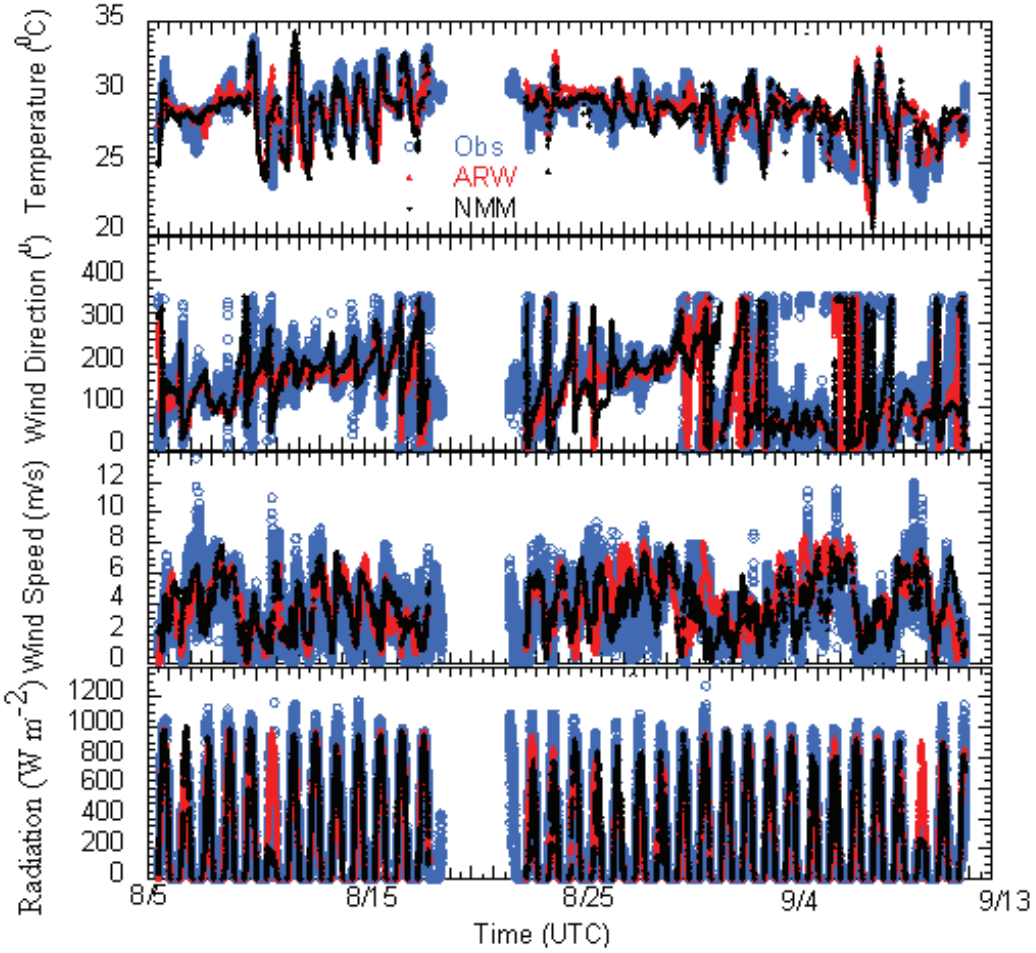

Figure 9. *Time–series of observations and model predictions (ARW and NMM) for meteorological parameters over the Gulf of Mexico on thebasis of ship measurements from 5 August to 13 September, 2006.*

Table 5. *Observations and models (NMM–CMAQ and ARW–CMAQ) for different gaseous species (O_3, CO, PAN, NOx, NO, NO_2, NO_y, ethylene, NO_z, Temperature (°C), wind speed (m/s) and direction, insolation (W/m^2) and NO_2+O_3 on the basis of ship measurements over the Gulf of Mexico during the 2006 TexAQS (all units are ppbv except meteorological parameters and PAN unit is pptv). Correlations between O_3 and NO_z for the NO_x–limited conditions indicated by the observational data with $(O_3)/(NO_x)$>46 (aged air masses) (see text for explanation)*

	Mean ± standard deviation			NMB (%)	
	Obs	**NMM–CMAQ**	**ARW–CMAQ**	**NMM–CMAQ**	**ARW–CMAQ**
CO	131.02±63.57	159.28±106.85	152.29±142.50	21.6	16.2
NO_y	14.88±73.51	18.94±26.91	16.22±27.28	27.3	9.1
O_3	36.38±24.13	40.07±22.46	41.33±20.36	10.1	13.6
NO	6.84±72.11	5.21±14.00	5.35±15.92	–23.8	–21.7
NO_2	6.32±10.39	12.33±17.95	9.15±14.75	95.3	45.0
NO_x	14.06±86.51	18.99±31.32	14.44±27.44	35.0	2.7
PAN	0.27±0.43	0.27±0.43	0.51±0.61	–41.5	91.6
NO_2+O_3	41.48±24.57	50.64±18.00	49.64±14.07	22.1	19.7
NO_z	2.34±3.77	6.21±6.71	3.87±3.86	64.9	164.7
Ethylene	1.81±4.53	0.97±1.73	0.76±1.25	–46.2	–57.8
Temperature	28.48±1.78	28.60±1.73	28.71±1.65	0.4	0.8
Wind Speed	3.51±1.87	3.88±1.75	4.12±1.93	10.5	17.4
Wind Direction	165.63±81.29	158.55±85.64	140.58±82.03	–4.3	–15.1
Insolation	503.93±326.25	513.18±309.29	533.03±307.44	1.8	5.8
Obs:	(O_3)=7.9(NO_z)+31.2	r=0.92			
ARW–CMAQ:	(O_3)=3.5(NO_z)+39.4	r=0.83			
NMM–CMAQ:	(O_3)=2.8(NO_z)+39.3	r=0.84			

Like the above analysis for the aircraft observations, the upper limits of ε_N values were estimated by the O_3–NO_z slope for the studied period over the Gulf of Mexico with the observed $(O_3)/(NO_x)$>46 during the daytime (6:00 am to 6:00 pm). A similar conclusion to that of the aircraft was obtained, i.e., the ε_N value of ARW–CMAQ (3.5) is slightly higher than NMM–CMAQ (2.8) and both are much lower than the observed value (7.9) as shown in Figure 8 and Table 5. This finding is not surprising due to the fact that the observations along the coast of southeastern Texas over the Gulf of Mexico on ship from August 5 to September 11 were just outside of the Houston–Galveston–Brazoria metropolitan area where most of aircraft measurements also took place as shown in Figure 2. Figure 9 shows that both models reproduced the temporal variations seen in the observed temperature, wind speed and direction, and insolation along the ship track most of time, especially for temperature.

The summary results of Table 5 show that the NMM model has the better performance for these meteorological parameters than the ARW model. In contrast to the results over the land on the basis of P–3 (see Table 4), the temperatures of both models are slightly higher than the observations and the mean temperature of the ARW model is slightly higher than that of the NMM model over the Gulf of Mexico as seen in Table 5. Figure 9 shows that most of the time both models reproduced the diurnal variations in the observed incoming solar radiation very well along the ship track, except peak of 8/10 (the NMM model seriously underestimated) and peak of 9/9 (the ARW model seriously overestimated). Spatial misplacements and irregularity of predicted cloud cover in both models resulted in the overestimations and underestimations of solar radiation (not shown).

4. Conclusions

A rigorous comparative evaluation of the impact of WRF–NMM and WRF–ARW meteorology on CMAQ simulation for O_3 and its related precursors has been carried over the eastern United States by comparing the model results with the intensive observations obtained during the 2006 TexAQS/GoMACCS campaign. Both models were used to provide the meteorological fields for the CMAQ simulations. The main conclusions of the evaluation are summarized. The comparisons with measurements at the AIRNow surface sites revealed that ARW–CMAQ and NMM–CMAQ have a very similar good performance for the high maximum 8–hr O_3 concentration range (>40 ppbv) with slightly better performance for ARW–CMAQ. The NMB values of ARW–CMAQ and NMM–CMAQ for the data with maximum 8–hr O_3>40 ppbv are 8.1% and 9.4%, respectively. Both models consistently overestimated the observations in the low O_3 concentration range (<40 ppbv) with NMB values of 38.9% (ARW–CMAQ) and 48.3% (NMM–CMAQ). On the basis of vertical profiles from NOAA P–3 aircraft over the Houston–Galveston–Brazoria and Dallas metropolitan areas, both models showed very similar performance for different chemical species (O_3, CO, PAN, NO_2, NO, NO_x, HNO_3, NO_y and ethylene) as both models use the same chemical mechanism and emission. NMM–CMAQ has slightly more overestimations for O_3, PAN, HNO_3, NO_z but slightly less overestimations for NO_x, NO, NO_2, and NO_y than ARW–CMAQ. On the other hand, both models reproduced the vertical variation patterns of the observed air temperature and water vapor well with the slightly lower mean values for the ARW–CMAQ model. This behavior is traced to difference in the initialization method used in the meteorological models.

The capability of both models to reproduce the observed pollutants along the coast of southeastern Texas over the Gulf of Mexico was found to be highly variable due to the fact that there were land–sea contrast, the sea–breeze circulation, land–use differences and along–shore coastal terrain irregularities. Both models captured, with a good deal of accuracy, the temporal variations and broad synoptic change seen in the observed O_3, NO_y, CO and O_3+NO_2 with the mean NMB value <25% along the ship track most of the time, although with some occasional major excursions. According to the ship data, NMM–CMAQ has slightly more overestimations for CO, NO_y, NO_2, NO_x but slightly less overestimations for O_3, NO_z, and PAN than ARW–CMAQ. Both models consistently underestimated NO and ethylene, suggesting that the models may have not included some emission sources of

NO and ethylene over the Gulf of Mexico. On the basis of O_3–NO_Z slope, the upper limits of the ozone production efficiency values for both aircraft and ship data were slightly lower for the NMM–CMAQ (2.7 to 2.8) than the ARW–CMAQ (3.4 to 3.5). In contrast to the results over the land on the basis of aircraft, the mean temperature of the ARW–CMAQ is slightly higher than the NMM–CMAQ over the Gulf of Mexico and both modeled temperatures are slightly higher than the observations. This behavior may be due to the fact that both models overestimated solar radiation [i.e. slightly higher NMB for ARW–CMAQ (5.8%) than NMM–CMAQ (1.8%)].

In light of the uncertainties in the photochemical mechanisms, prognostic model forecasts of meteorological fields and emissions, the overall performance of both models during the 2006 TexAQS/GoMACCS campaign can be considered to be reasonable. Given the fact that although WRF–ARW and WRF–NMM use different dynamic cores but are based on the same knowledge of state–of–science for the meteorological processes within the WRF framework, it is not surprising that ARW–CMAQ and NMM–CMAQ showed similar performance for O_3 and its related species. In fact, the reasonable performance of NMM–CMAQ is impressive as it is run in a real–time forecast mode for the national air quality forecasting.

Acknowledgements

The authors would like to thank J. Godowitch for the constructive and very helpful comments. We also thank Daiwen Kang, Daniel Tong, Jeff McQueen, Pius Lee, Youhua Tang, and Marina Tsidulko for collaboration and critical assistance in performing the forecast simulations. We are grateful to the 2006 TexAQS/GoMACCS investigators for making their measurement data available for verification of modeling results. The United States Environmental Protection Agency through its Office of Research and Development funded and managed the research described here. It has been subjected to Agency's administrative review and approved for publication.

References

Arnold, J.R., Dennis, R.L., Tonnesen, G.S., 2003. Diagnostic evaluation of numerical air quality models with specialized ambient observations: testing the Community Multiscale Air Quality modeling system (CMAQ) at selected SOS 95 ground sites. *Atmospheric Environment* 37, 1185-1198.

Banta, R.M., Senff, C.J., Nielsen-Gammon, J., Darby, L.S., Ryerson, T.B., Alvarez, R.J., Sandberg, S.P., Williams, E.J., Trainer, M., 2005. A bad air day in Houston. *Bulletin of the American Meteorological Society* 86, 657-669.

Bao, J.W., Michelson, S.A., McKeen, S.A., Grell, G.A., 2005. Meteorological evaluation of a weather-chemistry forecasting model using observations from the TEXAS AQS 2000 field experiment. *Journal of Geophysical Research-Atmospheres* 110, art. no. D21105.

Bernardet, L.R., Nance, L., Chuang, H.Y., Loughe, A., Demirtas, M., Koch, S., Gall, R., 2005. The developmental testbed center winter forecasting experiment. *Proceedings of 21st Conference on Weather Analysis and Forecasting/17th Conference on Numerical Weather Prediction*, American Meteorological Society, Paper 7.1, Washington, D.C.

Biswas, J., Rao, S.T., 2001. Uncertainties in episodic ozone modeling stemming from uncertainties in the meteorological fields. *Journal of Applied Meteorology* 40, 117-136.

Byun, D., Schere, K.L., 2006. Review of the governing equations, computational algorithms, and other components of the models-3 Community Multiscale Air Quality (CMAQ) modeling system. *Applied Mechanics Reviews* 59, 51-77.

Davis, J.M., Eder, B.K., Nychka, D., Yang, Q., 1998. Modeling the effects of meteorology on ozone in Houston using cluster analysis and generalized additive models. *Atmospheric Environment* 32, 2505-2520.

Eder, B., Kang, D.W., Mathur, R., Pleim, J., Yu, S.C., Otte, T., Pouliot, G., 2009. A performance evaluation of the National Air Quality Forecast Capability for the summer of 2007. *Atmospheric Environment* 43, 2312-2320.

Eder, B., Kang, D.W., Mathur, R., Yu, S.C., Schere, K., 2006. An operational evaluation of the Eta-CMAQ air quality forecast model. *Atmospheric Environment* 40, 4894-4905.

Eder, B.K., Davis, J.M., Bloomfield, P., 1994. An automated classification scheme designed to better elucidate the dependence of ozone on meteorology. *Journal of Applied Meteorology* 33, 1182-1199.

EPA., 1999. Guideline for Developing an Ozone Forecasting Program, EPA-454/R-99-009. Research Triangle Park, NC.

Federal Register, 2008. National Ambient Air Quality Standards for Ozone, ; Final Rule, Vol. 73, No. 60, Thursday, March 27, 2008, Rules and Regulations.

Gery, M.W., Whitten, G.Z., Killus, J.P., Dodge, M.C., 1989. A photochemical kinetics mechanism for urban and regional scale computer modeling. *Journal of Geophysical Research-Atmospheres* 94, 12925-12956.

Gilliam, R.C., Pleim, J.E., 2010. Performance assessment of new land surface and planetary boundary layer physics in the WRF-ARW. *Journal of Applied Meteorology and Climatology* 49, 760-774.

Janjic, Z.I., 2003. A nonhydrostatic model based on a new approach. *Meteorology and Atmospheric Physics* 82, 271-285.

Mathur, R., Shankar, U., Hanna, A.F., Odman, M.T., McHenry, J.N., Coats, C.J., Alapaty, K., Xiu, A.J., Arunachalam, S., Olerud, D.T., Byun, D.W., Schere, K.L., Binkowski, F.S., Ching, J.K.S., Dennis, R.L., Pierce, T.E., Pleim, J.E., Roselle, S.J., Young, J.O., 2005. Multiscale air quality simulation platform (MAQSIP): initial applications and performance for tropospheric ozone and particulate matter. *Journal of Geophysical Research-Atmospheres* 110, art. no. D13308.

Olszyna, K.J., Bailey, E.M., Simonaitis, R., Meagher, J.F., 1994. O_3 and NO_y Relationships at a Rural Site. *Journal of Geophysical Research-Atmospheres* 99, 14557-14563.

Otte, T.L., Pouliot, G., Pleim, J.E., Young, J.O., Schere, K.L., Wong, D.C., Lee, P.C.S., Tsidulko, M., McQueen, J.T., Davidson, P., Mathur, R., Chuang, H.Y., DiMego, G., Seaman, N.L., 2005. Linking the Eta Model with the Community Multiscale Air Quality (CMAQ) modeling system to build a national air quality forecasting system. *Weather and Forecasting* 20, 367-384.

Pagnotti, V., 1987. A meso-meteorological feature associated with high ozone concentrations in the northeastern United States. *JAPCA-the International Journal of Air Pollution Control and Hazardous Waste Management* 37, 720-722.

Pouliot, G., 2005. The emission processing system for the Eta/CMAQ air quality forecast system. *Presented at 85th American Meteorological Society Annual Meeting*, Paper 4.5, January 09-13, 2005, San Diego, CA.

Rogers, E., Black, T.L., Deaven, D.G., DiMego, G.J., Zhao, Q.Y., Baldwin, M., Junker, N.W., Lin, Y., 1996. Changes to the operational ''early'' Eta analysis/forecast system at the National Centers for Environmental Prediction. *Weather and Forecasting* 11, 391-413.

Skamarock, W.C., Klemp, J.B., Dudhia, J., Gill, D.O., Barker, D.M., Wang, W., Powers, J.G., 2005. A Description of the Advanced Research WRF Version 2. NCAR Technical Note NCAR/TND468+STR, http://www.mmm.ucar.edu/wrf/users/docs/arw_v2.pdf

Szoke, E., Koch, S.E., Barjenbruch, D., Wesley, D.A., 2007. Evaluation of the NCEP WRF NMM and ARW models for some recent high-impact weather events. *22nd Analysis and Forecasting/18th Conference on Numerical Weather Prediction*, American Meteorological Society, Paper 2A.6, Park City, Utah.

Wert, B.P., Trainer, M., Fried, A., Ryerson, T.B., Henry, B., Potter, W., Angevine, W.M., Atlas, E., Donnelly, S.G., Fehsenfeld, F.C., Frost, G.J., Goldan, P.D., Hansel, A., Holloway, J.S., Hubler, G., Kuster, W.C., Nicks, D.K., Neuman, J.A., Parrish, D.D., Schauffler, S., Stutz, J., Sueper, D.T., Wiedinmyer, C., Wisthaler, A., 2003. Signatures of terminal alkene oxidation in airborne formaldehyde measurements during TexAQS 2000. *Journal of Geophysical Research-Atmospheres* 108, art. no. 4104.

Wiedinmyer, C., Guenther, A., Estes, M., Strange, I.W., Yarwood, G., Allen, D.T., 2001. A land use database and examples of biogenic isoprene emission estimates for the state of Texas, USA. *Atmospheric Environment* 35, 6465-6477.

Yu, S., Mathur, R., Pleim, J., Pouliot, G., Wong, D., Eder, B., Schere, K., Gilliam, R., Rao, S.T., 2011. Comparative evaluation of the impact of WRF/NMM and WRF/ARW meteorology on CMAQ simulations for $PM_{2.5}$ and its related precursors during the 2006 TexAQS/GoMACCS study. *Atmospheric Chemistry and Physics Discuss* 11, 32031-32064.

Yu, S., Mathur, R., Schere, K., Kang, D., Pleim, J., Young, J., Tong, D., Pouliot, G., McKeen, S.A., Rao, S.T., 2008. Evaluation of real-time $PM_{2.5}$ forecasts and process analysis for $PM_{2.5}$ formation over the eastern United States using the Eta-CMAQ forecast model during the 2004 ICARTT study. *Journal of Geophysical Research-Atmospheres* 113, art. no. D06204.

Yu, S., Mathur, R., Schere, K., Kang, D., Pleim, J., Otte, T.L., 2007. A detailed evaluation of the Eta-CMAQ forecast model performance for O_3, its related precursors, and meteorological parameters during the 2004 ICARTT study. *Journal of Geophysical Research-Atmospheres* 112, art. no. D12S14.

Yu, S., Eder, B., Dennis, R., Chu, S.H., Schwartz, S.E., 2006a. New unbiased symmetric metrics for evaluation of air quality models. *Atmospheric Science Letters* 7, 26-34.

Yu, S., Mathur, R., Kang, D., Schere, K., Eder, B., Pleim, J., 2006b. Performance and diagnostic evaluation of ozone predictions by the Eta-community multiscale air quality forecast system during the 2002 New England Air Quality Study. *Journal of the Air and Waste Management Association* 56, 1459-1471.

Zhang, Y., Vijayaraghavan, K., Wen, X.Y., Snell, H.E., Jacobson, M.Z., 2009. Probing into regional ozone and particulate matter pollution in the United States: 1. A 1 year CMAQ simulation and evaluation using surface and satellite data. *Journal of Geophysical Research-Atmospheres* 114, art. no. D22304.